First attempts in 3D frequency-domain modelling of electromagnetic responses using eigenmodes

C. Stuntebeck, Institute of Geophysics and Meteorology, TU Braunschweig (c.stuntebeck@tu-bs.de)

Abstract

The utilization of free decay eigenmodes may be a promising approach to handle the computational work involved when modelling multi-frequency electromagnetic responses with high data density over three-dimensional conductors, as is substantial e.g. in airborne applications.

Each halfspace conductivity distribution owns a characteristic, continuous spectrum of free decay eigenfunctions and eigenvalues forming the decay constants. The electric eigenmodes in a conductor are governed by a homogeneous induction equation for the electric field, combined with the ansatz of an exponential decay with time. Outside the conductor the associated magnetic modes obey a potential field. Therefore, modes in the air are determined by field continuation of the magnetic modes at the earth's surface.

Even though the eigenmodes are constituted in time-domain, the frequency-domain electromagnetic responses of a conductor can be obtained by an expansion in terms of the eigenmodes, simply requiring the modes at positions of transmitter and receiver superposed with source dependent weights.

The defining equation for the electric eigenmodes is approximated using finite differences on a staggered grid spanning only the conductor. The air halfspace is treated by incorporating a surface integral-boundary condition. After finite-differencing, a sparse real-symmetric matrix system of equations is assembled. The large eigenvalue problem is solved using Sorensen's implicitly restarted Lanczos algorithm. The output is a discrete set of eigenmodes. In a first version of our modelling code, we have implemented the use of all eigenmodes for the field synthesis. For a modest sized grid, the code has been compared with the 1D analytical solution and produces results in very satisfactory agreement.

Unfortunately, for larger grids the memory requirements of the eigenvalue solver do not allow to simultaneously acquire all eigenmodes. One strategy to overcome this limitiation is to successively calculate small parts of the set of eigenmodes. This can only be achieved using a spectral transformation, which main drawback is the demand for the action of the shifted matrix **inverse** on a vector. In addition, the shifted matrix is indefinite and difficult to precondition for successful application of an iterative solver.

As a further improvement of the algorithm, ways of a proper partial synthesis using only few eigenmodes are discussed.

Introduction

The computational effort of 3D frequency-domain modelling is extremely high due to the fact that usually a large complex system of equations has to be solved many times for multiple soure locations and multiple frequencies. This applies for example to the finite differences implementation of Newman and Alumbaugh (1995) as well as to the code of Avdeev et al. (1998), which is based on the volume integral equation solution to Maxwell's equations. An important advance in modelling is suggested by Druskin and Knizhnerman (1994), who show that it is possible to obtain the multi-frequency responses at almost the computational cost for a single frequency using spectral Lanczos methods. The advantage of being able to solve efficiently for multiple frequencies is retained in the further development of the spectral Lanczos method (Druskin et al., 1999), but both still need to solve the system repeatedly for the source positions.

Our approach is to avoid this repetition by exploiting eigenmodes. The striking feature of free decay modes is their independence of any source. For a given conductivity distribution they have to be determined once only. This one set of eigenmodes then allows to obtain the responses of arbitrary measuring configurations and frequencies through ordinary superposition at low computational cost. However, the criticial point of this method is the effort which is necessary to aquire the set of eigenmodes.

In this paper we show how to simulate electromagnetic responses using eigenmodes which are determined by means of finite differences. First the theoretical basis concerning the properties of free decay modes and field continuation is compiled. Subsequently, a few notes regarding the practical implementation are given. We focus on symmetry and sparsity conservation when building the system matrix and a proper choice of the algorithm solving the resulting eigenvalue problem. The application of the method is then presented for a simple half-space model.

In the following, two aspects for the potential optimization of the method are evaluated: Numerical refinements when using the implicitly restarted Lanczos algorithm lead to the necessity of an iterative solver with an appropriate preconditioner. Secondly, we discuss the convergence behaviour of the superposition if only a limited number of modes is available.

Theoretical basics

Starting from Maxwell's equations in quasistatic approximation

$$\nabla \times \underline{E}(\underline{r}) = -\dot{\underline{B}}(\underline{r}), \tag{1}$$

$$\nabla \times \underline{B}(\underline{r}) = \mu_0 \left[\sigma(\underline{r})\underline{E}(\underline{r}) + \underline{J}_e(\underline{r})\right] \tag{2}$$

and after elimination of $\underline{B}$ the induction equation

$$\nabla \times \nabla \times \underline{E}(\underline{r}) + \mu_0 \sigma(\underline{r})\dot{\underline{E}}(\underline{r}) = -\mu_0 \dot{\underline{J}}_e(\underline{r}) \tag{3}$$

is obtained. In these expressions $\underline{E}$ and $\underline{B}$ are the vectors of the electric and magnetic field, and $\sigma(\underline{r})$ denotes the electrical conductivity as a function of position. $\underline{J}_e(\underline{r})$ is the source current density. The dotted variables signify time derivatives. In the absence of an exciting source the equation reduces to

$$\nabla \times \nabla \times \underline{E}(\underline{r}) + \mu_0 \sigma(\underline{r})\dot{\underline{E}}(\underline{r}) = 0. \tag{4}$$

The assumtion of an exponential decay with time of the electric field

$$\underline{E}(\underline{r}, t) = \underline{e}(\underline{r}) \exp(-\lambda t) \tag{5}$$

leads to the eigenvalue problem

$$\nabla \times \nabla \times \underline{e}(\underline{r}) = \lambda \mu_0 \sigma(\underline{r})\underline{e}(\underline{r}) \tag{6}$$

with the decay constant λ as eigenvalue for the spatial stationary eigenfunction $\underline{e}(\underline{r})$. Following Weidelt (1982, Appendix C) all solutions to (6) form an orthogonal set of vectorial eigenfunctions with $\sigma(\underline{r})$ as weighting function. Though the eigenvalue spectrum is continuous, the eigenvalues and -functions are denoted symbolically by discrete quantum numbers n and k. Then the orthogonality relation reads

$$\int_{\mathbb{R}^3} \sigma(\underline{r})\ \underline{e}_k(\underline{r})\underline{e}_n(\underline{r})\ \mathrm{d}^3\underline{r} = \delta_{kn} \tag{7}$$

and for $\sigma(\underline{r}) > 0$ the set forms a complete system. The field for any exitation in frequency-domain can be obtained by expanding $\underline{E}(\underline{r}, \omega)$ into a series of free decay modes (Weidelt, 1983, Appendix D)

$$\underline{E}(\underline{r}, \omega) = \underline{E}_\infty(\underline{r}, \omega) + \sum_n a_n(\omega)\ \underline{e}_n(\underline{r}) \tag{8}$$

with the source dependent weights

$$a_n(\omega) = \frac{-i\omega}{\lambda_n + i\omega} \int_{\mathbb{R}^3} \underline{J}^e(\underline{r}_0, \omega) \underline{e}_n(\underline{r}_0) \, \mathrm{d}^3\underline{r}_0 \tag{9}$$

and $\underline{E}_\infty(\underline{r}, \omega)$ accounting for the incompleteness of the expansion in the air, where $\sigma = 0$ is assumed. Remarkably, only eigenmodes at the positions of source $\underline{r}_0$ and receiver $\underline{r}$ do contribute to the expansion.

A similar relation can be derived for the magnetic field. Subsequently, we treat the case of a vertical magnetic dipole (VMD) at $\underline{r}_0$ with moment $m(\omega)$. The vertical component of its magnetic field response can be expressed by

$$B_{zz}(\underline{r}|\underline{r}_0, \omega) = B_{zz,\infty}(\underline{r}|\underline{r}_0) + \mu_0 m(\omega) \sum_n \frac{[\nabla \times \underline{e}_n(\underline{r})]_z \, [\nabla \times \underline{e}_n(\underline{r}_0)]_z}{\lambda_n + i\omega}, \tag{10}$$

where again $B_{zz,\infty}(\underline{r}|\underline{r}_0)$ accounts for the non-vanishing field in the air at the limit $\omega \to \infty$. Due to $[\nabla \times \underline{e}_n(\underline{r})]_z = -\dot{b}_{zn}(\underline{r})$ the vertical component of the time derivative of the magnetic eigenmodes $\dot{b}_{zn}$ may be substituted for the terms with the electric eigenmodes. Special care must be taken if source $\underline{r}_0$ and / or receiver $\underline{r}$ are situated in the air, since the eigenvalue equation (6) defines the electric eigenmodes only inside the conducting earth. Anyhow, to determine them is described in the following.

In the insulating air half-space, which is assumed to be at $z < 0$, holds

$$\nabla \times \underline{E} = -\dot{\underline{B}}, \tag{11}$$

$$\nabla \times \underline{B} = 0. \tag{12}$$

Therefore, $\dot{\underline{B}}$ is given by a scalar potential Ψ:

$$\dot{\underline{B}} = -\nabla \frac{\partial \Psi}{\partial z}. \tag{13}$$

Using $\nabla^2 \Psi = 0$, the potential may be determined by applying

$$-\nabla_H^2 \Psi = -\frac{\partial^2 \Psi}{\partial x^2} - \frac{\partial^2 \Psi}{\partial y^2} = \frac{\partial^2 \Psi}{\partial z^2} = \Psi'' \tag{14}$$

to all wanted discrete values $\Psi_p (p = 1, \ldots, P)$ of the potential in $z \leq 0$. Combining them to the vector of all potential values $\boldsymbol{\Psi} = [\Psi_1, \ldots, \Psi_P]^T$ and building $-\nabla_H^2 \boldsymbol{\Psi} = \boldsymbol{\Psi}''$ leads to the P-dimensional matrix system

$$\boldsymbol{F} \; \boldsymbol{\Psi}(z) = \boldsymbol{\Psi}''(z). \tag{15}$$

If $\mathbf{v}_j$ and η_j^2 are eigenvectors and eigenvalues of the problem $\boldsymbol{F} \; \mathbf{v}_j = \eta_j^2 \; \mathbf{v}_j$ it holds for $z \leq 0$

$$\boldsymbol{\Psi}(z) = \sum_{j=1}^{P} c_j \; \mathbf{v}_j \; \mathrm{e}^{\eta_j z}. \tag{16}$$

The coefficients c_j are set by the boundary values $\dot{\underline{B}}_z(z = 0) = -\boldsymbol{\Psi}''(z = 0)$, this yields

$$c_j = -\frac{1}{\eta_j^2} \; \mathbf{v}_j^{\mathrm{T}} \; \dot{\underline{B}}_z(z = 0), \quad \eta_j \neq 0. \tag{17}$$

To summarize, for $z < 0$ the magnetic field derivative $\dot{\underline{B}}(z)$ is defined completely by all the vertical components $\dot{B}_z(0)$ at the earth-air interface. This relation is valid also for the magnetic eigenmodes $\dot{\underline{b}}_n$ needed in the expansion (10) for the field of the VMD.

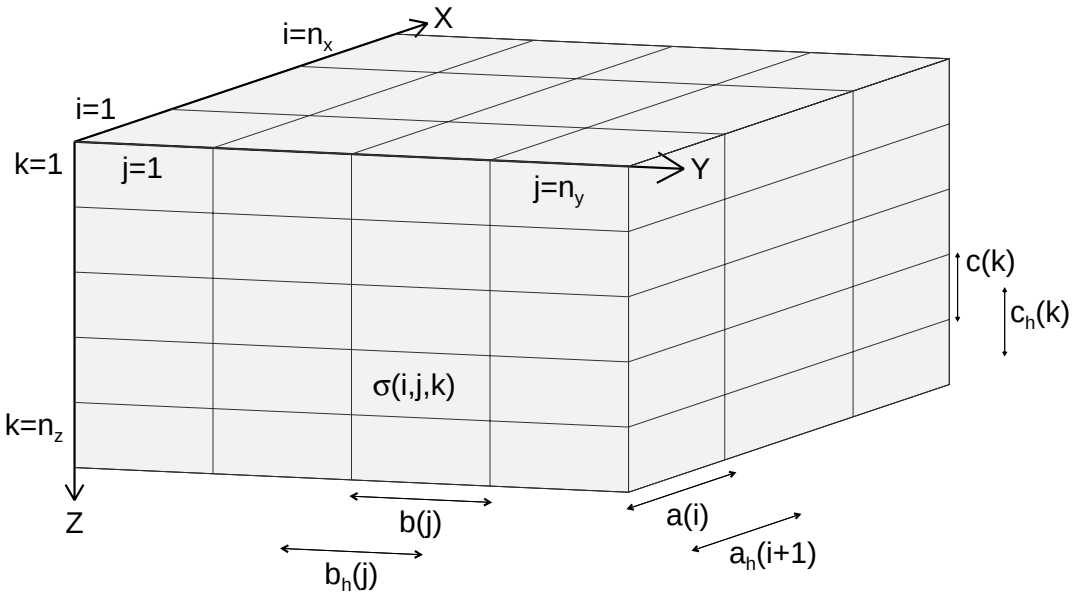

Figure 1: Schematic grid used for finite differencing.

Implementation

In order to solve the eigenvalue problem (6) numerically, we employ finite differences on a staggered grid, as sketched in Figure 1. The conducting subsurface is divided into $N_g = n_x n_y n_z$ regular cells with uniform conductivity $\sigma_n = \sigma(i,j,k)$ and volume $V_n = a(i)\ b(j)\ c(k)$, the cell edges are at $x(i)$, $x(i{+}1)$, $y(j)$, $y(j{+}1)$, $z(k)$ and $z(k{+}1)$. To each cell are assigned three electric and three magnetic eigenmode components, which are spread on the grid as outlined by Yee (1966). In the staggered arrangement (Figure 2) the magnetic eigenmode components are assigned to the

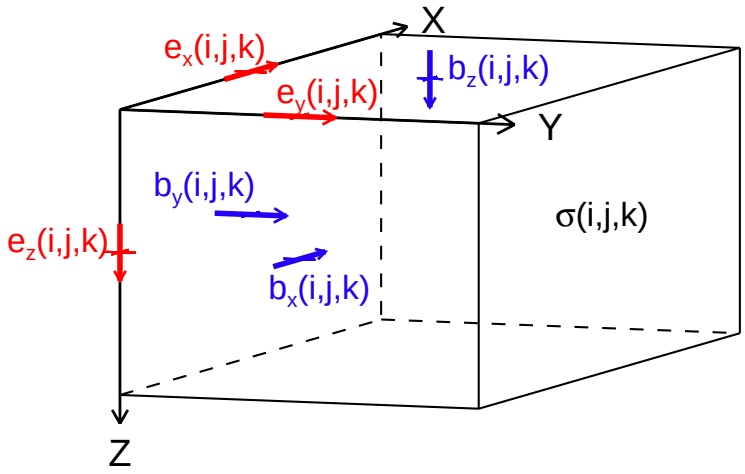

Figure 2: Yee grid of cell (i,j,k).

center of the faces of the cell and the electric ones to the edges. For simplicity, the components are numbered using only integer indices, namely those of the associated cell, though this does not reflect their actual coordinate on on the grid. For example $e_x(i,j,k)$ is located at coordinate $\{x_c(i), y(j), z(k)\}$, where $x_c(i) = [x(i{+}1) - x(i)]\,/2$. The distances between the midpoint coor-

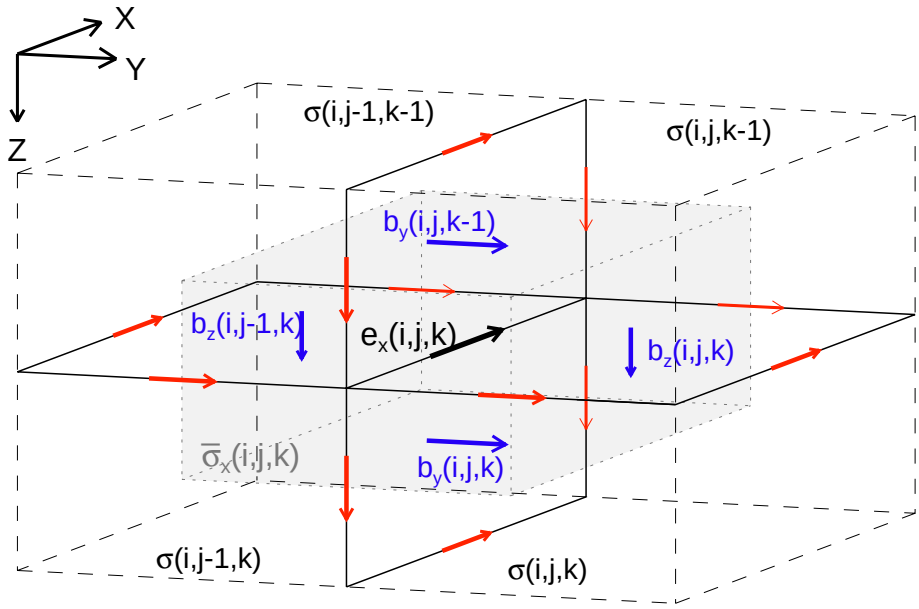

Figure 3: The grid cells and associated electric and magnetic components required for the FD equation of $e_x(i,j,k)$. The prism $p_x(i,j,k)$ with averaged conductivy $\bar{\sigma}_x(i,j,k)$ is shaded.

dinates $x_c(i)$, $y_c(j)$, $z_c(k)$ of cell (i,j,k) and its next neighbour in positive direction are labeled $a_h(i{+}1)$, $b_h(j{+}1)$, $c_h(k{+}1)$, and we define $a_h(1) = a(1)$, $a_h(n_x{+}1) = a(n_x)$ and the values in y and z direction respectively.

At the boundary to the air-halfspace, the grid is artificially extended half a cell height $c(1)/2$ into the air and missing values are replaced by those obtained using field continuation, which will be explained in detail below. The other five bounding walls of the grid are assumed to be perfectly conducting (Dirichlet boundary conditions), which demands vanishing tangential components of the electric eigenmodes.

When establishing the finite difference version of the eigenvalue problem, it is necessary to employ spatial averages of the conductivities to take into account the differences resulting from the placement of the electric components on different edges of the cell. We integrate over a prism centered around each electric component and calculate the volume-weighted arithmetic average of the conductivity of the surrounding cells along the current path. The average conductivity $\bar{\sigma}_x$ associated with e_x of cell (i,j,k) for example is (see also Figure 3)

$$\bar{\sigma}_x(i,j,k) = \frac{1}{4p_x(i,j,k)} \left\{ \begin{array}{l} b(j)\,c(k)\,\sigma(i,j,k) \;+\; b(j{-}1)\,c(k)\,\sigma(i,j{-}1,k) \\ +\, b(j{-}1)\,c(k{-}1)\,\sigma(i,j{-}1,k{-}1) \;+\; b(j)\,c(k{-}1)\,\sigma(i,j,k{-}1) \end{array} \right\}, \qquad (18)$$

where $p_x(i,j,k) = a(i)\,b_h(j)\,c_h(k)$ is the prism used for integration. The finite difference approximation of (6) for component e_x of cell (i,j,k) then can be written as

$$\frac{\dot{b}_z(i,j,k) - \dot{b}_z(i,j{-}1,k)}{b_h(j)} - \frac{\dot{b}_y(i,j,k) - \dot{b}_y(i,j,k{-}1)}{c_h(k)} = -\lambda\,\mu_0\,\bar{\sigma}_x(i,j,k)\,e_x(i,j,k), \qquad (19)$$

where $\dot{b}_z$ and $\dot{b}_y$ have to be replaced by the finite difference version of $\underline{\dot{b}} = -\nabla \times \underline{e}$, for example

$$\dot{b}_z(i,j,k) = -\frac{e_y(i{+}1,j,k) - e_y(i,j,k)}{a(i)} + \frac{e_x(i,j{+}1,k) - e_x(i,j,k)}{b(j)}. \qquad (20)$$

From (19) and (20) it is apparent that each electric component inside the grid is connected with only twelve surrounding electrical components. Therefore, setting up the equations for all electric components on the grid yields a matrix system with no more than 13 entries per row. The matrix symmetry is conserved by the transformation

$$\tilde{e}_x(i,j,k) = \sqrt{\mu_0\, p_x(i,j,k)\, \bar{\sigma}_x(i,j,k)}\; e_x(i,j,k), \tag{21}$$

which mainly contains the square root of the average conductivity and the volume of the integration prism belonging to the respective eigenmode component. Similarly, the transformation has to be performed for the e_y and e_z components.

The ideal sparse structure of the matrix is disturbed for the horizontal components of the first grid layer ($k=1$), where the boundary condition introduces additional elements into the system matrix. Namely, instead of applying an equation like (20) to replace the magnetic eigenmode component which is situated in the air-halfspace, as $\dot{b}_y(i,j,k{-}1)$ in the above example, it is determined using field continuation. Following (13), (16) and (17), the field continuation of one magnetic component needs all $\dot{b}_z(i,j,k=1)$ at the grid surface. Or, expressing the continuation solely through electric eigenmodes using (20) shows that all horizontal electric eigenmodes e_x and e_y with $k=1$ do contribute. This leads to a dense submatrix for the $N_h = n_x\,(n_y{-}1) + (n_x{-}1)\,n_y$ nontrivial horizontal electric eigenmode components of the top cells. Excluding the vanishing tangential eigenmode components at the perfectly conducting walls, the total numer of nontrivial electric eigenmode components is

$$N = n_x(n_y{-}1)n_z + (n_x{-}1)n_y n_z + (n_x{-}1)(n_y{-}1)n_z. \tag{22}$$

The matrix form of the eigenvalue problem with dimension N reads

$$\boldsymbol{A}\ \mathbf{x} = \lambda\ \mathbf{x}, \tag{23}$$

where $\mathbf{x}$ is the vector of all electric eigenmode components. It seems to be advantageous to

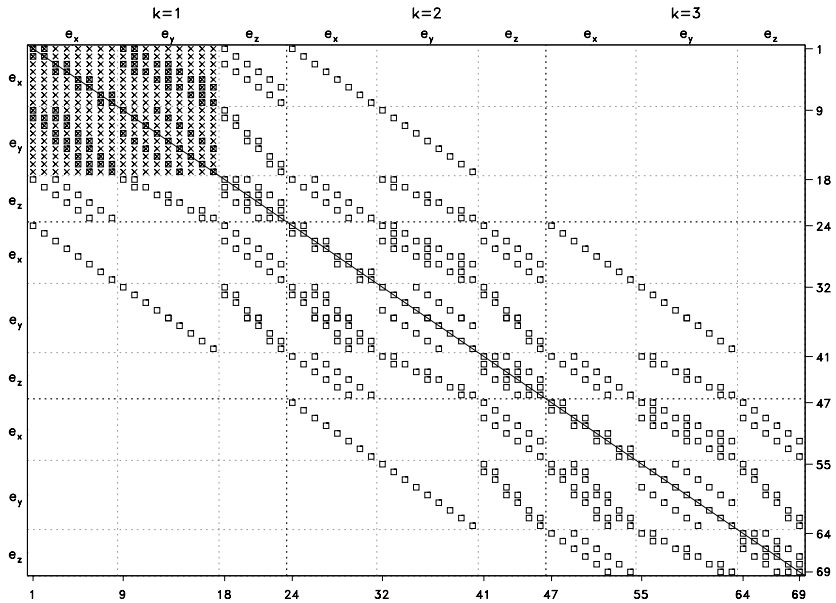

Figure 4: Sparsity structure of the matrix associated with a small $4 \times 3 \times 3$ grid. The dimension of the matrix is $N = 69$, the FD non-zero elements are represented by squares and the elements due to field continuation are marked with $\times$.

order the components in the vector with depth, thus assembling all e_x, e_y, e_z for one layer before proceeding to the next deeper one. The sparsity structure of the complete system matrix $\boldsymbol{A}$ is illustrated in Figure 4. The matrix $\boldsymbol{A}$ has the properties of being real, symmetric, positiv-semidefinite, high-dimensional ($N \approx 3N_g$) and sparse with predominantly 13 entries per row or column. Only the matrix' non-zero elements are stored using a Compressed Sparse Row (CSR) storage scheme (see e.g. Saad (1995)), which does not account for the symmetry, but was chosen because it is commonly used in sparse matrix software like SPARSKIT (Saad, 1994). This public domain code is used to efficiently perform some of the required standard matrix operations.

Solving the posed large eigenvalue problem with direct methods like Householder reduction to tridiagonal form and suitable factorization does not account for the sparsity of the matrix and becomes not feasible when the grid size is increased. Established algorithms to specifically treat large, sparse eigenvalue problems are provided by the software package ARPACK (Lehoucq et al., 1998). Thereof the Implicitly Restarted Lanczos Method (IRLM) is used to determine the set of N eigenvalues λ_n and eigenvectors $\mathbf{x}_n$ of our system matrix.

To model the frequency response of the conductor, merely a small part of each eigenvector, namely $\mathbf{x}_n^h = [x_{n,1}, \ldots, x_{n,N_h}]^T$, is needed: Since the synthesis (10) needs the magnetic eigenmodes only at the measuring positions, for airborne applications it is sufficient to store for each of the N eigenvalues the corresponding N_h horizontal electric eigenmodes at the surface. All other $N \cdot (N{-}N_h)$ components at gridpoints inside the conductor are disregarded.

When the superposition of eigenmodes is carried out, for better convergence it is favourable to separate the magnetostatic part ($\omega{=}0$) of the field. Instead of (10), the synthesis reads

$$B_{zz}(\underline{r}|\underline{r}_0,\omega) = B_{zz,\infty}(\underline{r}|\underline{r}_0) + B_{zz,0}(\underline{r}|\underline{r}_0) + \mu_0 m(\omega) \sum_n \frac{-i\omega}{\lambda_n(\lambda_n + i\omega)} \dot{b}_{zn}(\underline{r})\dot{b}_{zn}(\underline{r}_0), \qquad (24)$$

where $B_{zz,0}(\underline{r}|\underline{r}_0) = \mu_0 m(\omega) \sum_n \frac{1}{\lambda_n} \dot{b}_{zn}(\underline{r})\dot{b}_{zn}(\underline{r}_0)$ denotes the separated magnetostatic field part. The expression $B_{zz,\infty}(\underline{r}|\underline{r}_0) + B_{zz,0}(\underline{r}|\underline{r}_0)$ is calculated analytically through superposition of the VMD magnetostatic fields of the source and it's mirror source, which is reflected at the boundary to the perfectly conducting halfspace at depth $z(n_z{+}1)$.

Verification of code

In order to verify the accuracy of our eigenmode modelling, the responses of a simple model have been compared to the semi-analytic layered half-space solution (see e.g. Ward and Hohmann (1988), pp. 208). Here we consider a uniform half-space of 100 Ωm. The earth is divided into $16 \times 16 \times 8 = 2048$ cells using a regular 160 m × 168 m × 25 m grid. The number of unknown electric eigenmodes is $N{=}5640$. Their eigenvalue spectrum ist is represented in Figure 5. Striking characteristic of the spectrum is that about 1/3 of the eigenvalues is equal to zero, and their respective eigenmodes do not contribute to the synthesis. It can be shown that this property applies to arbitrary conductivity allocation to the cells and that the number of zero eigenvalues is equivalent to the number of vertical electric eigenmodes e_z, which is $N_v = (n_x{-}1)(n_y{-}1)n_z$. Subsequently, only the positive eigenvalues need to be determined. To give an idea how the eigenmodes look like, the modes at the earth's surface associated with the six smallest positive eigenvalues are illustrated in Figure 6. In this example, the eigenmodes show nice symmetry reflecting the homogeneity of the subsurface. Adherence of the boundary conditions can be observed for e_x and e_y. The vertical magnetic eigenmode calculated from the electric ones sometimes vanishes for all surface gridpoints, as it occurs here for the eigenvalues with number 1801, 1803 and 1805. Again, those modes yield no contribution to the field synthesis but their occurence could not yet be generalized.

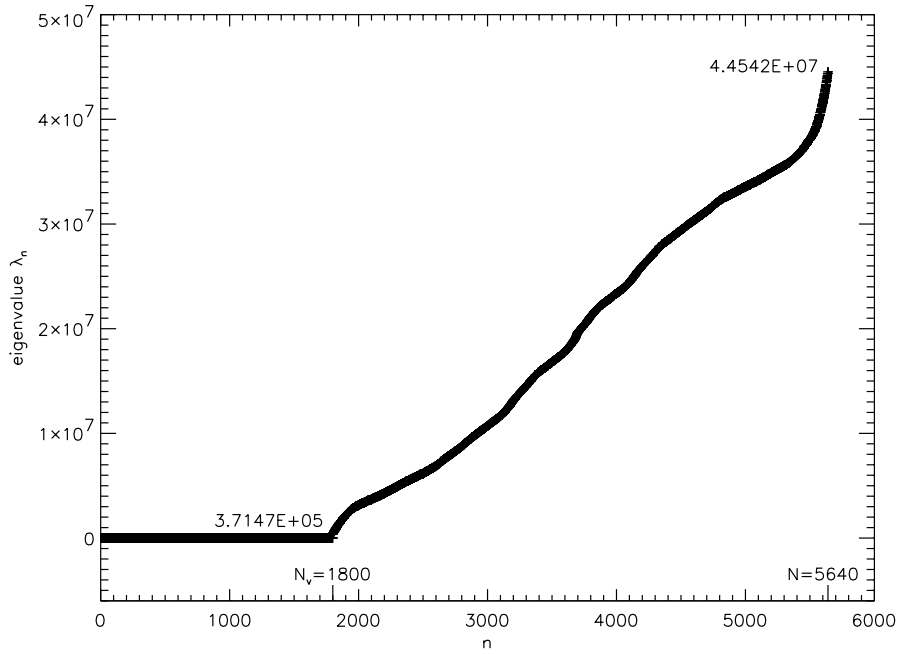

Figure 5: Eigenvalue spectrum of 100 Ωm half-space constisting of 2048 cells.

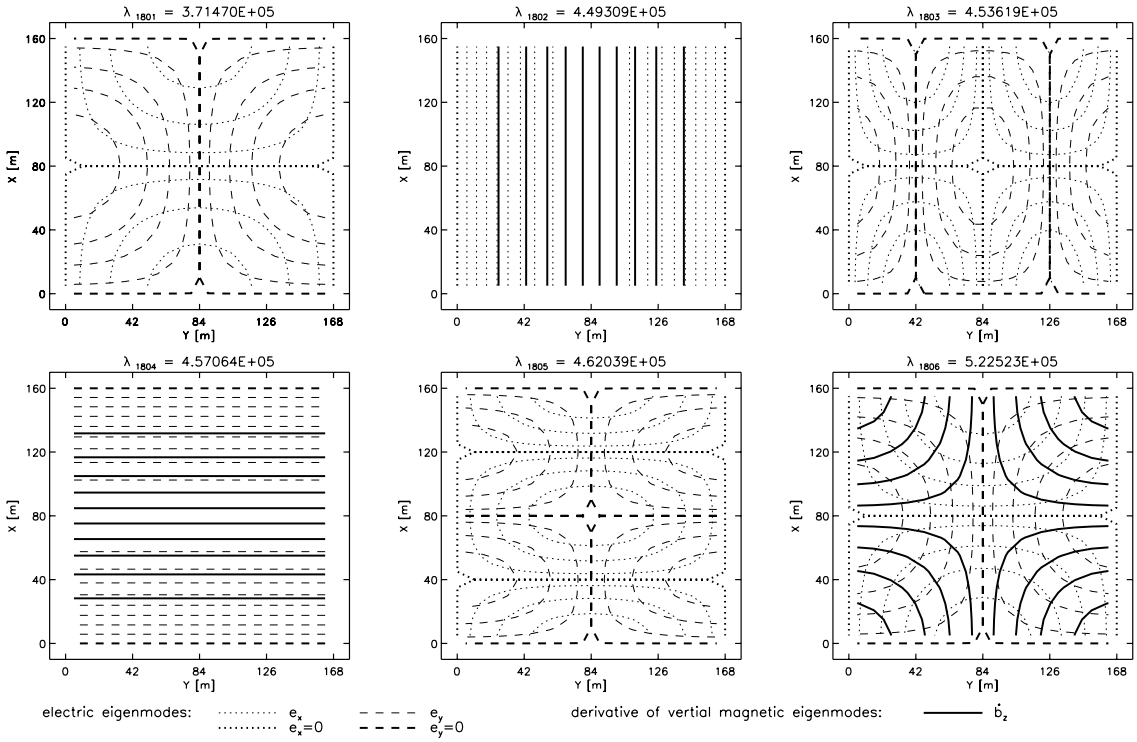

Figure 6: Eigenmodes at the earth's surface belonging to the six smallest positive eigenvalues of 100 Ωm half-space constisting of 2048 cells.

For a VMD operating at a frequency of 8.6 kHz, the responses obtained using the 3D eigenmode synthesis, as defined in equation (24), are shown in Figure 7. Transmitter and receiver are kept at fixed distance ($r = 10\,\mathrm{m}$) and are moved along a line in x-direction, which is positioned at $y = 84\,\mathrm{m}$ at the earth's surface. The real and imaginary parts of the modelled secondary field show good agreement with the reference 1D semi-analytical solution. Similar good results are

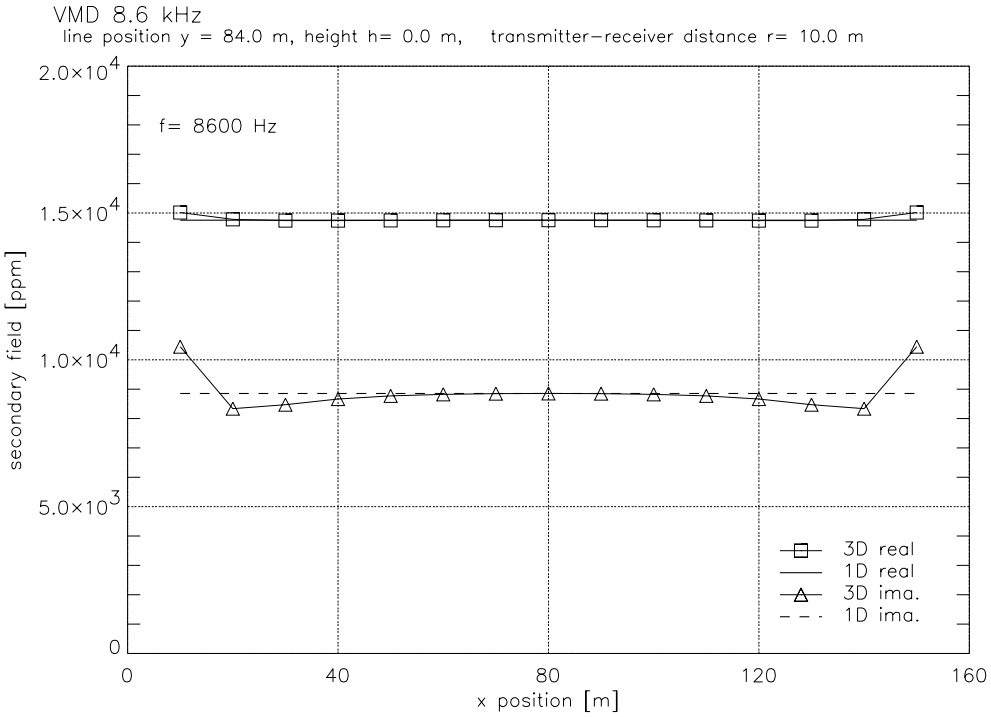

Figure 7: VMD fields of 3D eigenmode synthesis compared to 1D semi-analytical solution for a 100 Ωm half-space.

accomplished performing the synthesis at height h above the surface. Though, due to the field continuation, side effects propagate more to the interior of the grid.

The same set of eigenmodes has been used to simulate the VDM responses over a wide frequency range from $f_{min} = 380$ Hz to $f_{max} = 192$ kHz. The respective skin depths range from $p_{max} = 258$ m to $p_{max} = 11.5$ m. For the latter, the request on the maximum cell dimension d to be $d \leq p/3$ is fulfilled only in vertical direction. Nevertheless, the synthesis (Figure 8) yields acceptable results for all frequencies.

Having presented the promising capabilities of the eigenmode approach we now need to contrast the computational effort of the method. The storage requirements soon exceed the memory available on today's normal PCs or workstations. For the above treated grid, the 3840 non-zero eigenmodes already claim 165 Mb for storage, additional twice the amount has to be reserved to be able to determine the modes. On an 'alphaserver' (883 MHz), the execution time for determination of all non-zero eigenmodes is 3.5 h, whereas the synthesis for five frequencies at 15 positions takes only a few seconds.

Optimization possibilities

The approximate eigenvalue problem solvers provided by ARPACK require $N \cdot \mathcal{O}(K) + \mathcal{O}(K^2)$ memory storage locations when K is the number of eigenvalues to be computed of the N-dimensional matrix. Whereas N is predetermined by the employed grid, the number K may be arbitrarily chosen to match the available memory. Therefore, one conceivable strategy to overcome memory limitations is to sucessively calculate parts of the set of eigenmodes, each of size K. Since the implemented Krylov method allows to calculate only eigenvalues from either end of the spectrum, to acquire those eigenvalues from the interior of the spectrum a spectral transformation is inevitable. The shift and invert spectral transformation mode solves the

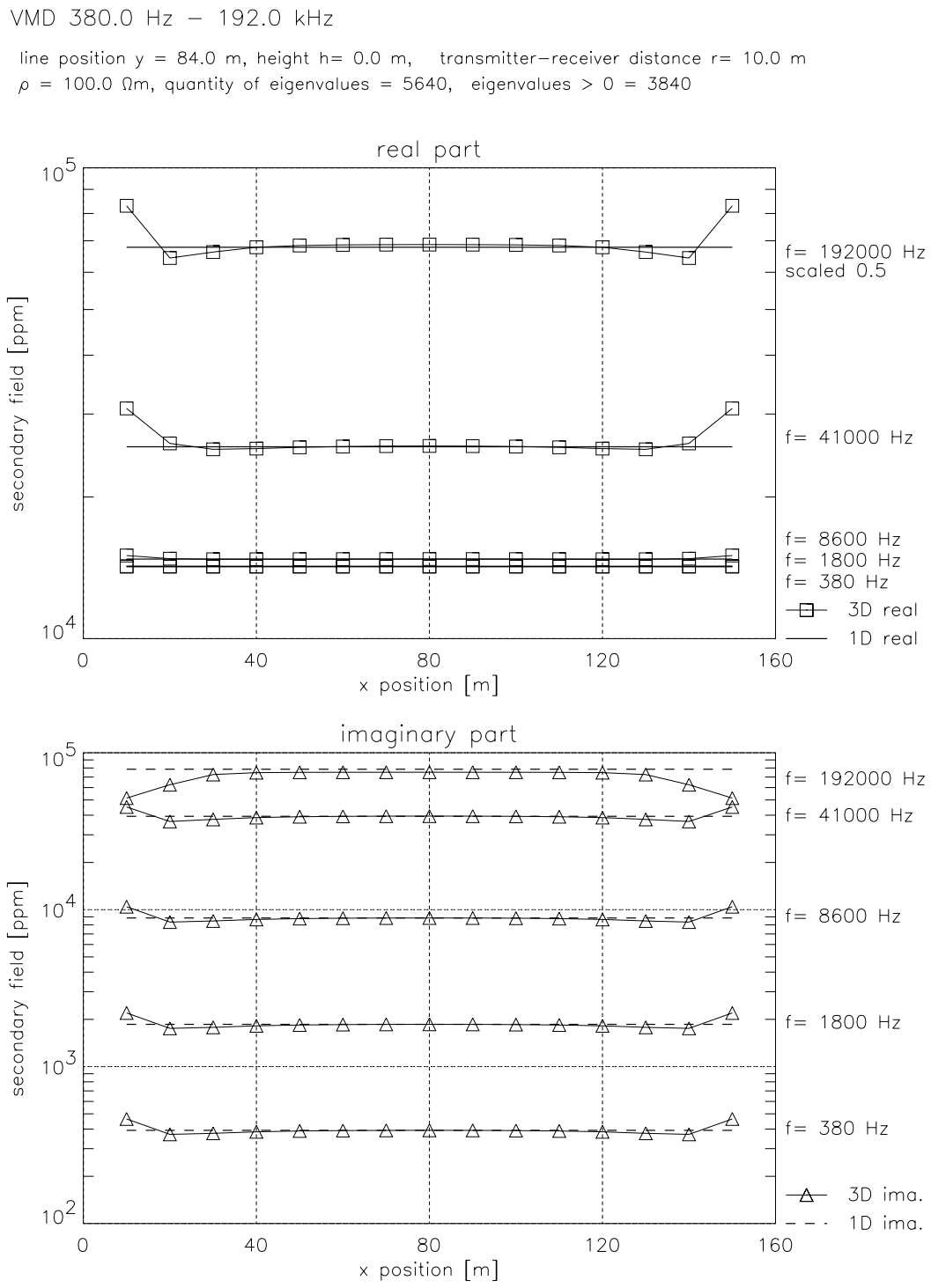

Figure 8: VMD fields for various frequencies, responses of 3D eigenmode synthesis compared to 1D semi-analytical solution over a 100 Ωm half-space.

modified eigenvalue problem

$$(\boldsymbol{A} - \delta \boldsymbol{I})^{-1}\ \mathbf{x} = \nu\, \mathbf{x}\ ,\ \text{where}\ \nu = \frac{1}{\lambda - \delta}. \tag{25}$$

Hereof, the K largest eigenvalues ν_k are obtained and transformed back to eigenvalues of the original problem using

$$\lambda_k = \delta + \frac{1}{\nu_k}, \tag{26}$$

yielding the K smallest original eigenvalues which are larger than the shift δ. Through successivly increasing the shift δ, the determination of any desired portion of the spectrum can be accomplished, at least theoretically. Some precaution with this approach has to be taken regarding the preservation of the orthogonality between all eigenmodes, which is essential for a successful field synthesis.

In practice, to calculate the action of the shifted matrix inverse on a vector causes some difficulties. For any positive shift δ the system matrix becomes indefinite which restricts the choice of an iterative solver, e.g. the well-known conjugate gradient technique cannot be applied. We have tested several of the general iterative methods and preconditioners provided as templates by Barrett et al. (1994) without satisfactory results. Especially designed for indefinite, but symmetric systems are the algorithms SYMMLQ and MINRES. We have implemented SYMMLQ (Paige and Saunders, 1975) as iterative solver and obtained acceptable convergence rates for small positive shifts δ. However, for shifts between the smallest and largest eigenvalue, the iterative solver does not converge anymore (see Figure 9), if no preconditioning is applied. When preconditioning indefinite systems, most of the standard techniques do not work: For example, using SYMMLQ with simple Jacobi scaling as preconditioner increases the number of iterations to more than twice the quantity needed without. Similar poor results yields the application of SSOR or several variants of the incomplete Cholesky/LU decomposition preconditioner as provided by Saad (1994).

Recently, we have implemented a preconditioner suggested by Gill et al. (1992), which is based on a modification of the Bunch-Parlett factorization of a matrix $\tilde{\boldsymbol{A}}$ that somehow approximates

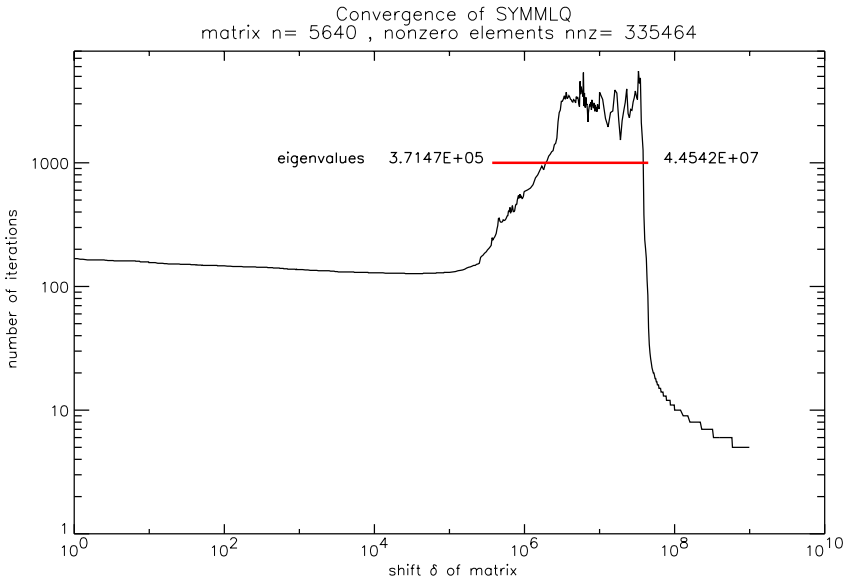

Figure 9: Number of iterations needed by SYMMLQ depending on the shift δ of the system matrix $\boldsymbol{A}$ when no preconditioning is applied.

$\boldsymbol{A}$. The factorization is calculated using the sparse implementation provided in the Harwell code MA27 (HSL, 2002). With the 'exact' Bunch-Parlett preconditioner, calculated from $\tilde{\boldsymbol{A}} \equiv \boldsymbol{A}$, SYMMLQ solves the system $(\boldsymbol{A} - \delta \boldsymbol{I})^{-1}\ \mathbf{y} = \mathbf{z}$ at at most three iterations, independently of the value of the shift. But this procedure is less reasonable, since the work building the preconditioner exceeds the work necessary to directly solve the system using the original Bunch-Parlett factorization. One of our next tasks will be the search for a matrix with clever affinity to $\boldsymbol{A}$, yielding an elaborate preconditioner at affordable cost.

Another way to reduce the computational effort may be the application of an approximate synthesis which is accomplished with only part of eigenmodes, namely those with smallest positive eigenvalues. The sum over all eigenmodes in (24) can be decomposed in terms with different powers of $1/\lambda_n$:

$$\sum_n \frac{-i\omega}{\lambda_n(\lambda_n + i\omega)} = \sum_n \left(\frac{-i\omega}{\lambda_n^2} + \frac{-\omega^2}{\lambda_n\,(\lambda_n^2 + \omega^2)} + \frac{i\omega^3}{\lambda_n^2\,(\lambda_n^2 + \omega^2)} \right). \tag{27}$$

The first addend describes the frequency-proportional part of the field, which may possibly be replaced by an expression calculated from an equivalent source current system in the conductor. The remaining sum contains the inverse eigenvalues with dominant powers of three and higher. A fast convergence of the sum is expected, where only the smallest positive eigenvalues and their respective eigenmodes do contribute significantly to the field synthesis. The convergence behaviour has to be investigated for various conductivity distributions, aiming at finding an appropriate truncation criterion.

Concluding remarks

A 3D frequency-domain EM modelling code has been developed on the basis of free decay modes in the conductor. Expressing the governing equations and boundary conditions in terms of finite differences leads to a sparse real-symmetric system matrix of high dimension. The large eigenvalue problem is solved using an implicitly restarted Lanczos algorithm in shift and invert mode. As iterative solver the SYMMLQ algorithm has been employed since it was judged to be one of the best available for matrix systems that are indefinite but symmetric.

The performance of the new modelling method is demonstrated for a simple half-space model and modest sized grid. The complete set of non-zero 3D eigenmodes is used to obtain the EM responses of the conductor for a broad frequency range. Comparison with the semi-analytic 1D solution shows that our results are in acceptable to good agreement. One important attribute of the method is that it yields the multi-frequency and multi-position responses in a straightforward manner once the eigenmodes are known. At present, unfortunately this advantage is almost nullifed by the computational work necessary to determine the eigenmodes.

We plan to increase the efficiency of the code by both reducing the quantity of necessary eigenmodes as well as the effort to determine each mode. The latter may be achieved by implementing an appropriate preconditioner for the shifted matrix, whereupon the modified Bunch-Parlett factorization seems to be most auspicious so far.

Acknowledgements

I would like to thank P. Weidelt for his suggestion and encouraging support of the work as well as for contributing some constitutive parts of the code. To the authors of the used numerical software packages I want to express my appreciation for freely distributing their programs on the World Wide Web, which was of great benefit to the progress of the work. The project is funded by the Deutsche Forschungsgemeinschaft (WE 1048/7-1).

References

Avdeev, D. B., Kuvshinov, A. V., Pankratov, O. V. and Newman, G. A., 1998. Three-dimensional frequency-domain modeling of airborne electromagnetic responses. *Exploration Geophysics* **29**, 111–119.

Barrett, R., Berry, M., Chan, T. F., Demmel, J., Donato, J., Dongarra, J., Eijkhout, V., Pozo, R., Romine, C. and der Vorst, H. C., 1994. *Templates for the Solution of Linear Systems: Building Blocks for Iterativ Methods*. SIAM, Philadelphia, PA.
URL `http://www.netlib.org/templates/Templates.html`

Druskin, V. and Knizhnerman, L., 1994. Spectral approach to solving three-dimensional diffusion Maxwell's equations in the time and frequency domains. *Radio Science* **29**, 937–953.

Druskin, V. L., Knizhnerman, L. A. and Lee, P., 1999. New spectral Lanczos decomposition method for induction modeling in arbitrary 3-D geometry. *Geophysics* **64(3)**, 701–706.

Gill, P. E., Murray, W., Ponceleon, D. B. and Saunders, M. A., 1992. Preconditioners for indefinite systems arising in optimization. *SIAM J. Matrix Anal. Appl.* **13**, 292–311.

HSL, 2002. A collection of Fortran codes for large scale scientific computation.
URL `http://www.numerical.rl.ac.uk/hsl`

Lehoucq, R. B., Sorensen, D. C. and Yang, C., 1998. *ARPACK Users' Guide: Solution of Large-Scale Eigenvalue Problems with Implicitly Restarted Arnoldi Methods*. SIAM, Philadelphia, PA.
URL `http://www.caam.rice.edu/software/ARPACK/`

Newman, G. A. and Alumbaugh, D. L., 1995. Frequency domain modelling of airborne electromagnetic responses using staggered finite differences. *Geophysical Prospecting* **43**, 1021–1042.

Paige, C. C. and Saunders, M. A., 1975. Solution of sparse indefinite systems of linear equations. *SIAM J. Numer. Anal.* **12**, 617–629.
URL `http://www.stanford.edu/~saunders/symmlq/f77/`

Saad, Y., 1994. SPARSKIT: A basic tool kit for sparse matrix calculations, Version 2. Technical report, CSRD, University of Illinois and RIACS (NASA Ames Research Center).
URL `http://www.cs.umn.edu/research/arpa/SPARSKIT/sparskit.html`

Saad, Y., 1995. *Iterative methods for sparse linear systems*. PWS Publishing Company, Boston.

Ward, S. H. and Hohmann, G. W., 1988. Electromagnetic Theory for Geophysical Applications. In M. N. Nabighian (editor), *Electromagnetic Methods in Applied Geophysics - Theory*, volume 1, Society of Exploration Geophysicists, Tulsa, Oklahoma.

Weidelt, P., 1982. Response characteristics of coincident loop transient electromagnetic systems. *Geophysics* **47**, 1325–1330.

Weidelt, P., 1983. The harmonic and transient electromagnetic response of a thin dipping dike. *Geophysics* **48**, 934–952.

Yee, K. S., 1966. Numerical solution of initial boundary problems involving Maxwell's equations in isotropic media. *IEEE Trans. Ant. Propag.* **14**, 302–309.